International Journal of Cardiology 274 (2019) 388–393

Contents lists available at ScienceDirect

International Journal of Cardiology

journal homepage: www.elsevier.com/locate/ijcard

Accuracy of cadmium-zinc-telluride imaging in detecting single and multivessel coronary artery disease: Is there any gender difference?☆

Alessia Gimelli [a,1], Nicola Riccardo Pugliese [b,*,1], Annette Kusch [a], Assuero Giorgetti [a], Paolo Marzullo [a,c]

[a] Fondazione Toscana G. Monasterio, Pisa, Italy
[b] Cardio-Thoracic and Vascular Department, University Hospital of Pisa, Pisa, Italy
[c] CNR, Institute of Clinical Physiology, Pisa, Italy

ARTICLE INFO

Article history:
Received 31 July 2018
Received in revised form 24 September 2018
Accepted 25 September 2018
Available online 28 September 2018

Keywords:
Myocardial perfusion imaging
Cadmium-zinc-telluride
Coronary artery disease
Multi-vessel disease
Women

ABSTRACT

Purpose: To evaluate gender-related differences in diagnostic accuracy of cadmium-zinc-telluride (CZT) myocardial perfusion imaging in detecting single- and multi-vessel coronary artery disease (CAD).
Methods: We prospectively enrolled 1161 consecutive patients with known or suspected coronary artery disease (288, 25% women and 873, 75% men) who had been referred to our laboratory for stress–rest myocardial perfusion imaging (single-day stress–rest protocol, mean radiation dose: 4 mSv). All patients underwent coronary angiography within 30 days; significant CAD was defined in the presence of a coronary stenosis >70%. Summed stress scores (SSS), summed rest scores (SRS) and summed difference scores (SDS) were obtained. Image quality was graded "good" or better in >90% of patients.
Results: On coronary angiography, left main trunk, left anterior descending artery, left circumflex artery and right coronary artery obstructive stenosis were seen in 13, 486, 393 and 499 patients, respectively. Global SSS was the best predictor of CAD in women (AUC = 0.866, 81% sensitivity and 79% specificity) and in men (AUC = 0.871, 76% sensitivity and 84% specificity). Interestingly, its accuracy was maintained also in patients with two-vessel (women: AUC = 0.842, $p < 0.001$; men: AUC 0.839, $p < 0.001$) or three-vessel disease (women: AUC = 0.800, $p < 0.001$; men: AUC 0.804, $p < 0.001$). There was no gender-related difference in terms of diagnostic accuracy.
Conclusions: Evaluation of multivessel disease can be obtained by CZT camera in men as well as in women, with high accuracy at a lower radiation exposure.

1. Introduction

Ischaemic heart disease (IHD) is frequently related to the presence of coronary artery disease (CAD), and the worst prognosis is associated to the presence of a multi-vessel disease [1]. CAD is characterized by a different gender distribution, with a higher prevalence in males than females. Epidemiology has influenced trial designs in the past, with the result of a lower amount of studies including women, in comparison to men [1]. Recent studies in large cohorts of women undergoing single photon emission computed tomography (SPECT) myocardial perfusion imaging (MPI) have shown a significant accuracy of the technique in terms of both diagnostic and prognostic applications [2–4]. However, reported SPECT accuracy in detecting multi-vessel CAD remains lower in comparison to single-vessel CAD, above all in women [5–7]. The reason why SPECT can miss high-risk CAD is probably related to the concept of balanced ischemia, due to flow-limiting three-vessel CAD or left main stenosis [8]. In this scenario, the introduction of dedicated cardiac cameras, equipped with solid state cadmium-zinc-telluride (CZT) detectors, has allowed a multiparametric evaluation of cardiac perfusion and function with a significant reduction in acquisition time and injected dose [9,10]. The increase in spatial and temporal resolution could improve the sensitivity and specificity of MPI in detecting multivessel disease, but confirming data from large populations (including women) are lacking [11–14]. Aim of this study was to evaluate, in patients with known or suspected CAD, the accuracy of CZT-based MPI in detecting one-vessel, two-vessel and three-vessel disease, using coronary angiography as the reference standard, and to demonstrate, if present, gender-related differences in each subgroup of CAD.

2. Methods

Between January 2010 and December 2016, we prospectively enrolled a group of 1161 consecutive patients (873 men, 75.2%) admitted for known or suspected CAD, referred to our Institution for stress–rest MPI obtained by CZT camera and who underwent invasive coronary angiography up to one month after the evaluation of ischaemia, irrespective of MPI findings. Patients with acute or recent (<three months) myocardial infarction and unstable angina were excluded from the study. The study was approved

☆ All authors take responsibility for all aspects of the reliability and freedom from bias of the data presented and their discussed interpretation

* Corresponding author at: Fondazione CNR/Regione Toscana "Gabriele Monasterio", via Moruzzi n.1, CNR Research Area, 56124 Pisa, Italy.
E-mail address: n.r.pugliese88@gmail.com (N.R. Pugliese).

[1] Equally contributed to this study as first co-authors.

https://doi.org/10.1016/j.ijcard.2018.09.102
0167-5273/

by the local ethics committee. All subjects gave written informed consent in accordance with the declaration of Helsinki.

2.1. Stress protocols

Patients were instructed to discontinue beta-blockers, calcium antagonists and nitrates 48 h before testing. A bicycle exercise stress test (stepwise increments of 25 W every min) or dipyridamole (intravenous administration of 0.56 mg/kg over 4 min) was chosen in 775 (66.6%) and 386 (33.2%), respectively. Adverse events were defined according to international guidelines [15].

2.2. Acquisition protocol

Patients underwent stress/rest CZT scintigraphy (Discovery NM 530c; GE Healthcare, Haifa, Israel) according to a single-day protocol with the administration of 148–185 MBq of ^{99m}Tc-tetrofosmin during stress and 296–370 MBq at rest (mean radiation dose for the complete protocol: 4 mSv) [6]. In all patients, CZT imaging was performed 15 min after stress injection of the radiopharmaceutical (^{99m}Tc-tetrofosmin) with an acquisition time of 7 min. A submaximal exercise was defined by inability to reach 85% of the age-predicted maximum heart rate or a rate pressure product of 26,000, in absence of stress-induced severe chest pain and/or significant ST-segment depression. We included in the study patients capable of achieving at least 80% of the age-predicted maximum heart rate, as internal clinical practice of our laboratory [4]. Patients were injected at rest, 30 min after the end of the first acquisition and then, after an interval of 30–45 min, a second acquisition was carried out for 6 min [16]. Patients were imaged in the supine position with arms placed over their head without any detector or collimator motion. All images were acquired with a 32 × 32 matrix and a 20% energy window centred at the 140 keV photopeak of ^{99m}Tc (pixel width 4 mm). Images were reconstructed on a standard workstation (Xeleris II; GE Healthcare, Haifa, Israel) without scatter or attenuation correction.

2.3. Analysis of CZT images

The quality of both stress and rest images was graded visually on a four-point scale as 1 (poor), 2 (fair), 3 (good) or 4 (excellent). The following parameters were considered: myocardial count density and uniformity; endocardial and epicardial edge definition; visualization; and background noise, especially from the subdiaphragmatic area. Stress and rest perfusion images from the CZT camera were semiquantitatively scored according to the 17-segment model of the left ventricle [17] and a five-point scale (0 normal, 1 equivocal, 2 moderate and 3 severe reduction in radioisotope uptake, and 4 absence of detectable tracer uptake). Then, summed stress score (SSS), summed rest score (SRS) and summed difference score (SDS) were calculated. To match the results with coronary angiograms, the 17 segments were grouped into territories of the three main coronary arteries, as previously outlined [17]: left anterior descending artery (LAD), circumflex artery (LCx) and right coronary artery (RCA). A random sample of 5% of patients was re-analysed by two experienced nuclear cardiologists, performing both qualitative and semiquantitative analysis independently. The readers were blinded to the coronary anatomy but not to the clinical information; consensus was reached on all analyses.

Left ventricular volume, ejection fraction and mass were measured after stress and at baseline using previously validated software (Xeleris IV; GE Healthcare, Haifa, Israel) [18]. Moreover, the same software automatically fits the LV volume curve with a fourth-order harmonic function in order to derive the peak filling rate (PFR, end-diastolic volume $* s^{-1}$) as an indicator of LV diastolic function, as previously described [10,19]. Finally, LV eccentricity index (EI) was evaluated as a sign of LV remodeling using a dedicated software (QGS/QPS; Cedars-Sinai Medical Center, CA, USA). LV EI varies from 0 (sphere) to 1 (line) and it is calculated from the major axis (Rz) and the minor axes (Rx and Ry) of the ellipsoid that best fits the mid- myocardial surface of the LV, according to the following formula: $EI = [1 - (RxRy/Rz^2)]^{0.5}$ [20].

2.4. Coronary angiography

Selective conventional coronary angiography was performed using standard techniques (Innova 2000 GE; General Electric). Coronary angiograms were quantitatively analysed using an off-line computer-based software program (MEDIS CMS version 6.0; MEDIS Imaging Systems) with an automatic edge-contour detection algorithm. The variables explored were the presence of significant stenosis (≥70% luminal diameter reduction) in the epicardial coronary arteries or ≥50% in the left main trunk. According to the number of the involved coronary arteries, we described one-vessel, two-vessel and three-vessel CAD; left main trunk stenosis ≥50% was considered as two-vessel CAD.

2.5. Statistical analysis

Continuous measures were expressed as the mean value ± SD or median and interquartile range for normally and skewed distributed variables, respectively. Continuous variables from 2 sets of data were compared using Student's *t*-test or Mann-Whitney *U* test when distribution was not normal. Categorical variables were presented as percentages and were compared using the Chi-square test. ANOVA or Kruskal-Wallis test were used to test differential distribution of data among >2 groups, with appropriate post-hoc corrections for interactions, i.e. Tukey-Kramer or Conover test, respectively. Intra-observer and inter-observer variability were measured using percent agreement and kappa values. Accuracy in coronary stenosis detection was assessed by receiver operating characteristic (ROC) analysis, reporting areas under the curve (AUCs) and their associated 95% confidence intervals (CIs). The best value in the prediction of CAD was defined as the cut-off point having the highest Youden index (sensitivity + specificity − 1). A p value < 0.05 was used to define statistical significance. The analyses were carried out with SPSS version 23.0 (IBM Corp., Armonk, NY).

3. Results

Table 1 summarizes the clinical characteristics of the general population. The most common cardiovascular risk factor was arterial hypertension, both in men and in women. Four-hundred-eighty-two patients (42%) had a history of angina pectoris, while the rest of the population showed atypical angina (305 patients, 26%) or effort dyspnoea (374 patients, 32%). We observed 13 left main trunk stenosis, 486 LAD stenosis, 393 LCx stenosis and 499 RCA stenosis. Absence of significant coronary stenosis was detected in 417 (36%) patients.

3.1. Image quality and evaluation of semiquantitative scores

Stress images were graded "good" or better in 1070/1161 patients (92%), and rest images in 1045/1161 patients (90%). No differences were observed in image quality between men and women. The intra-observer and inter-observer variability of qualitative analysis were 92% (kappa 0.87, 95% CI 0.73–0.93) and 88% (kappa 0.78, 95% CI 0.71–0.91), respectively. For the semiquantitative scores, the intra-observer and inter-observer variability were 88% (kappa 0.80, 95% CI 0.68–0.91) and 83% (kappa 0.74, 95% CI 0.65–0.89), respectively.

3.2. MPI analysis in the overall population

MPI protocol and cardiac functional parameters are summarized in Table 1. Median SSS and SRS were significantly higher in men than in women ($p < 0.01$), while no difference in SDS was noted. Male patients were characterized by higher LV volumes, a greater LV mass index (LVMi), a lower EF and a worse diastolic function, both at rest and after stress, together with a more advanced LV remodeling, expressed by a lower LV EI (all $p < 0.001$). There was not a gender-related distribution of myocardial stunning (248 patients, 21.4%), defined as a decrease >5% of LV EF after stress.

3.3. MPI analysis according to the number of vessels with CAD

In women (Table 2), perfusion data (SRS, SSS and SDS) showed a significant and coherent increasing trend in relation to the number of diseased vessels (from one-vessel to three-vessel CAD, all $p < 0.001$). SSS was the only parameter able to detect a significant distinction between two-vessel and three-vessel CAD. About morpho-functional analysis, a significant increasing trend in relation to the number of diseased vessels was observed for LVMi, EF (after stress), and LV volumes, with a reduced PFR (both at rest and after stress) and a higher percentage of myocardial stunning in women with multi-vessel CAD (all $p < 0.05$). In men (Table 2), all the parameters were significantly different in relation to the number of diseased vessels. Notably, SSS and SRS were able to discern significantly between two-vessel and three-vessel CAD.

3.4. Diagnostic accuracy of MPI according to the number of vessel with CAD

ROC curves with global SSS in female and male patients to predict involvement of at least one vessel (AUC = 0.866, 0.821–0.903 and AUC = 0.871, 0.837–0.893), two vessels (AUC = 0.842, 0.795–0.883 and AUC = 0.839, 0.813–0.863) and three vessels (AUC = 0.800, 0.749–0.844 and AUC = 0.804, 0.748–0.839) are shown in Fig. 1 A, B, C ($p < 0.001$ for all the AUCs). The statistical model provided the same cut-off for women and men both in two-vessel (SSS > 9) and three-vessel CAD (SSS > 11), differently from one-vessel disease (SSS > 6 in

Table 1
Characteristics of the population.

Variable	Total population ($n = 1161$)	Women ($n = 288$)	Men ($n = 873$)	p-Value
Demographics				
Age	71.1 (70.3–71.7)	72.2 (70.9–73.1)	70.7 (69.7–71.5)	ns
BSA	1.96 (1.94–1.97)	1.80 (1.78–1.84)	1.99 (1.98–2.01)	<0.001
Sinus rhythm	961 (82)	240 (82.8)	721 (81.7)	ns
Atrial fibrillation	162 (13.8)	44 (15.2)	118 (13.4)	ns
Paced rhythm	49 (4.2)	12 (4.1)	37 (4.2)	ns
Cardiovascular risk factors				
Family history of CVD	330 (28.4)	95 (33)	235 (26.9)	0.048
Smoking	119 (10.2)	22 (7.6)	97 (11.1)	ns
Diabetes mellitus	377 (32.5)	79 (27.4)	298 (34.1)	0.035
Arterial hypertension	701 (60.4)	182 (63.2)	519 (59.5)	ns
Dyslipidaemia	498 (42.9)	115 (39.9)	383 (43.9)	ns
Previous MI	253 (21.8)	46 (16)	207 (23.7)	0.006
Previous PCI/CABG	133 (11.5)	29 (10.1)	104 (11.9)	ns
Coronary anatomy				
CAD	744 (64.1)	157 (54.5)	587 (67.2)	<0.001
1-vessel CAD	330 (28.4)	66 (22.9)	264 (30.2)	0.017
2-vessel CAD	222 (19.1)	47 (16.3)	175 (20)	ns
3-vessel CAD	192 (16.5)	44 (15.3)	148 (17)	ns
MPI protocol				
Exercise RPP ($*10^3$)	23.5 (19.6–26.7)	20.5 (16.8–23.7)	24.5 (21.7–26.9)	0.001
Dipyridamole RPP ($*10^3$)	12 (11.4–12.9)	12 (11–13.9)	12 (11.5–13.1)	ns
Positive stress ECG	237 (20.4)	57 (19.8)	180 (20.6)	ns
Perfusion data				
Summed rest score	2 (1–3)	1 (1–2)	3 (2–4)	<0.001
Summed stress score	8 (7–9)	7 (6–8)	8 (8–9)	0.002
SSS LAD	3 (2–4)	2 (2–3)	3 (3–4)	ns
SSS LCX	2 (1–3)	2 (2–3)	2 (2–3)	ns
SSS RCA	2 (1–3)	1 (1–2)	3 (2–4)	0.007
Summed difference score	5 (4–6)	5 (4–6)	5 (4–6)	ns
LV volume and function at rest				
Ejection fraction (%)	59 (58–60)	65 (64–67)	57 (56–58)	<0.001
End-diastolic volume index (mL/m^2)	51.5 (50.3–52.9)	43.7 (41.9–45.8)	54.8 (53.1–56.7)	<0.001
End-systolic volume index (mL/m^2)	22.5 (21.8–23.4)	17.6 (16.3–19.2)	24.1 (22.9–25.5)	<0.001
LV eccentricity index	0.88 (0.87–0.89)	0.89 (0.89–0.90)	0.87 (0.86–0.88)	<0.001
Peak filling rate (EDV/s)	2.34 (2.28–2.40)	2.55 (2.44–2.66)	2.29 (2.22–2.34)	<0.001
LV mass index (g/m^2)	72.7 (71.6–74)	69.3 (68.2–71.2)	74.4 (72.7–75.5)	<0.001
LV volume and function after stress				
Ejection fraction (%)	58 (57–59)	66 (64–68)	56 (55–57)	<0.001
End-diastolic volume index (mL/m^2)	50.9 (49.6–52.5)	42.8 (40.9–44.6)	53.8 (52.2–55.1)	<0.001
End-systolic volume index (mL/m^2)	21.5 (23.5)	17.9 (16.6–20.2)	23.9 (22.6–25.3)	<0.001
Peak filling rate (EDV/s)	2.31 (2.20–2.37)	2.50 (2.32–2.66)	2.29 (2.17–2.34)	0.004
Myocardial stunning[a] (%)	248 (21.4)	61 (21.2)	187 (21.4)	ns

Data are presented as number and %, mean and 95% confidence interval if normally distributed or median and 95% confidence interval if not normally distributed. BSA: body surface area; CABG: coronary artery by-pass graft; CAD: coronary artery disease (at least one vessel with a luminal diameter stenosis >70%); CT: computed tomography; CVD: cardiovascular disease; EDV: end-diastolic volume; LAD: left anterior descending artery; LCX: left circumflex artery; LMCA: left main coronary artery; LV: left ventricle; MI: myocardial infarction; PCI: percutaneous coronary intervention; RCA: right coronary artery; RPP: rate pressure product; SSS: summed stress score.

[a] Defined as number of patients with >5% decrease in LV ejection fraction.

women and SSS > 7 in men). In each subgroup, pairwise comparison between the AUCs obtained from ROC analysis in women and men demonstrated no significant difference, as demonstrated by pairwise comparison between sensitivity and specificity in the same subgroups (Table 3). Likewise, there was no difference in diagnostic accuracy between one-, two- and three-vessel CAD both in women and in men (p = ns between subgroups).

Considering only women without CAD ($n = 131$), 103 (78.6%) showed SSS ≤6, while 28 (21.4%) had SSS > 6. The latter subgroup was characterized by a significantly older age (73.1 ± 6.7 vs 67.7 ± 10.3 years old; p = 0.01), with a higher proportion of dyslipidaemia (19/103, 18.5% vs 12/28, 43%; p = 0.03) and history of previous MI (2/103, 1.9% vs 4/28, 14.3% p = 0.02). Similarly, among 286 men without CAD, 45 (15.7%) had SSS > 7 (p = 0.04 vs women): compared to subgroup with SSS ≤ 7 (241/286, 84.3%), these patients had a significantly higher proportion of arterial hypertension (29/45, 64.5% vs 108/241, 44.8%; p = 0.03).

4. Discussion

The analysis of a large population of consecutive patients with known or suspected CAD demonstrated a high accuracy of MPI in detecting CAD, with the possibility of correctly identifying also multivessel disease with satisfactory sensitivity and specificity. These results are confirmed in a large sample of women ($n = 228$, 25% of the overall population), traditionally depicted as delicate patients.

MPI is a pivotal technique for the non-invasive evaluation of myocardial perfusion [21], but its underperformance in the event of diffuse CAD with balanced reduction of myocardial blood flow (i.e. three-vessel disease or left main trunk stenosis) is frequently described. Actually, several other reasons for mismatch MPI-angiography can be cited, e.g. insufficient coronary vasodilation (ingestion of caffeine-containing products), attenuation/motion artefacts, the absence of functional measurement of the stenosis by invasive angiography or the existence of coronary microvascular disease [22]. In our study,

Table 2
Cardiac functional parameters according to the number of vessels with CAD in women and men.

Women (n = 288)	No CAD (n = 131)	1-vessel CAD (n = 66)	2-vessel CAD (n = 47)	3-vessel CAD (n = 44)	p-Value
Perfusion data					
Summed rest score	0 (0–0)	2 (1–3.4)^	3 (2–4)^	5 (3–6)^,*	<0.001
Summed stress score	3 (3–4)	8 (8–9)^	12 (10.9–14.1)^,*	15 (12–17)^,*,§	<0.001
SSS LAD	1 (0–1.3)	3 (0.5)^	5.7 (4.2–7.2)^,*	6 (5–8)^,*,§	<0.001
SSS LCX	1 (1–2)	3 (2–4.2)^	4 (3–5)^	5 (4–6)^,*	<0.001
SSS RCA	0 (0–1)	0.5 (0–2.9)	3.4 (2.6–4.3)^,*	4.4 (3.5–5.3)^,*	<0.001
Summed difference score	2 (2–3)	5 (4.6–7)^	7.9 (6.6–9.1)^,*	8.5 (7.2–9.7)^,*	<0.001
LV structure and function					
Ejection fraction at rest (%)	66 (64–68)	65.5 (61–69)	63.8 (59.6–68.1)	59.3 (53.9–64.6)	ns
End-diastolic volume index at rest (mL/m^2)	41.4 (39.6–43.7)	42.9 (39.1–46)	47.2 (42.9–51.4)	50.5 (46.1–58)^,*	0.02
End-systolic volume index at rest (mL/m^2)	15.6 (14–17.1)	17.7 (15.1–21.5)	21.1 (15.3–23.9)	22.8 (19–36.5)^,*	0.002
LV eccentricity index at rest	0.90 (0.89–0.91)	0.89 (0.88–0.90)	0.89 (0.88–0.91)	0.84 (0.80–0.88)	ns
Peak filling rate at rest (EDV/s)	2.81 (2.66–2.88)	2.50 (2.23–2.66)^	2.40 (2.17–2.65)^	2.18 (1.95–2.40)^,*	<0.001
LV mass index at rest (g/m^2)	68.1 (65.5–70.6)	70.7 (67.9–75.2)^	69.8 (66.2–75)	71.8 (81.3)^	0.02
Ejection fraction after stress (%)	67 (65–69)	65 (62–69)	64.3 (60–68.5)	56.8 (51.4–62.3)^,*	0.04
End-diastolic volume index after stress (mL/m^2)	40.9 (39.5–42.8)	43.1 (39.6–46)	46.8 (38.7–53.1)	52.9 (45.9–58.7)^,*	0.007
End-systolic volume index after stress (mL/m^2)	15.8 (13.6–17.6)	17.9 (15.2–21.9)^	21.9 (16.4–25.1)^	25.3 (20.3–37.3)^,*	<0.001
Peak filling rate after stress (EDV/s)	2.88 (2.57–3.01)	2.45 (2.12–2.58)^	2.31 (2.00–2.58)^	2.05 (1.69–2.42)^	<0.001
Myocardial stunning[a]	18 (13.7)	19 (19.7)	12 (25.5)	15 (34.1)	0.04
Men (n = 873)	No CAD (n = 286)	1-vessel CAD (n = 264)	2-vessel CAD (n = 175)	3-vessel CAD (n = 148)	p-Value
Perfusion data					
Summed rest score	0 (0–0)	3 (2–3.4)^	5 (4–6)^,*	8 (5–10)^,*,§	<0.001
Summed stress score	4 (4–4)	8 (8–9)^	13 (12–14)^,*	16 (13–18)^,*,§	<0.001
SSS LAD	0 (0–1)	3 (2–4)^	6 (5–6.2)^,*	7 (6–8)^,*,§	<0.001
SSS LCX	2 (0–2)	2 (1–2)	4 (3–5)^,*	5 (4–5)^,*,§	<0.001
SSS RCA	1 (0–1)	2 (0–4)^	4.7 (4.2–5.2)^,*	5 (4–5)^,*	<0.001
Summed difference score	3 (3–3)	5 (4–5)^	7.2 (6.7–7.7)^,*	7 (6–8)^,*	<0.001
LV volume and function					
Ejection fraction at rest (%)	61 (59.5–62)	56 (55–57)^,*	56 (53–58)^	52 (48.8–55.2)^,*	<0.001
End-diastolic volume index at rest (mL/m^2)	51.4 (49.4–54.3)	56.4 (53.5–59)^	55.1 (51–58.9)^	59.1 (54.6–65.7)^	<0.001
End-systolic volume index at rest (mL/m^2)	20.8 (20.1–22.8)	24.5 (23.1–27)^	24.8 (22.6–28.9)^	27.9 (24.5–32.5)^	<0.001
LV eccentricity index at rest	0.88 (0.88–0.89)	0.87 (0.85–0.88)^	0.84 (0.82–0.85)^	0.85 (0.80–0.87)^	<0.001
Peak filling rate at rest (EDV/s)	2.40 (2.32–2.47)	2.28 (2.15–2.37)^	2.21 (2.1–2.31)^	2.11 (1.97–2.34)^	<0.001
LV mass index at rest (g/m^2)	70.8 (68.9–73)	75.8 (73.7–78.1)^	75.6 (72.1–77.8)^	77.4 (73.5–82)^	<0.001
Ejection fraction after stress (%)	59 (58–60)	56 (55–58)^	53 (50.8–56)^,*	49.5 (46–54)^,*	<0.001
End-diastolic volume index after stress (mL/m^2)	50.6 (48.5–52.7)	54.7 (52.3–58.6)^	55.5 (53.3–58.7)^	60.1 (52.2–64.2)^	<0.001
End-systolic volume index after stress (mL/m^2)	21.2 (20.1–22.5)	24.1 (22.1–26.6)^	26.4 (23.3–29.5)^	28.6 (24.9–35.3)^,*	<0.001
Peak filling rate after stress (EDV/s)	2.63 (2.52–2.75)	2.25 (2.12–2.35)^	2.16 (2.03–2.29)^	1.95 (1.8–2.1)^,*	0.004
Myocardial stunning[a]	44 (15.4)	52 (19.7)	42 (24)	45 (30.4)	0.002

Data are presented as number and %, mean and 95% confidence interval if normally distributed or median and 95% confidence interval if not normally distributed. CAD: coronary artery disease; EDV: end-diastolic volume; LV: left ventricle; SSS: summed stress score.
[a] Defined as number of patients with >5% decrease in LV ejection fraction.
^ $p < 0.05$ in comparison with no CAD.
* $p < 0.05$ in comparison with 1-vessel CAD.
§ $p < 0.05$ in comparison with 2-vessel CAD.

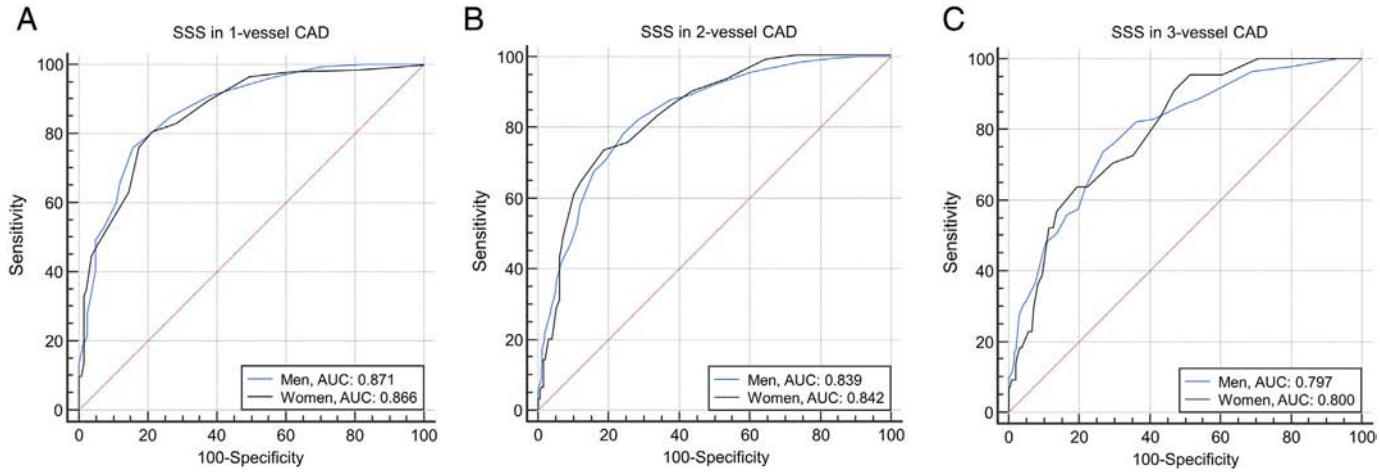

Fig. 1. Receiver operating characteristic curve analysis in women (black line) and men (blue line) according to the presence of one-vessel (A), two-vessel (B) and three-vessel CAD (C). The curves represent for each SSS cut-off point pairs of sensitivity–specificity values. CAD: coronary artery disease; SSS: summed stress score.

Table 3
Diagnostic accuracy of MPI-derived SSS in women and men according to the number of vessels with CAD.

	Women					Men					p^ value
	Cut-off	SEN (95% CI)	SPE (95% CI)	AUC (95% CI)	p* value	Cut-off	SEN (95% CI)	SPE (95% CI)	AUC (95% CI)	p* value	
1-vessel CAD	>6	80.8 (73.7–86.6)	78.6 (70.6–85.3)	0.866 (0.821–0.903)	<0.001	>7	75.9 (72.2–79.3)	84.2 (79.4–88.2)	0.871 (0.847–0.893)	<0.001	ns
2-vessel CAD	>9	73.3 (63–82.1)	81.2 (75.1–86.4)	0.842 (0.795–0.883)	<0.001	>9	78.3 (73.4–82.8)	75.7 (71.9–79.3)	0.839 (0.813–0.863)	<0.001	ns
3-vessel CAD	>11	63.6 (47.8–77.6)	80.7 (75.1–85.4)	0.800 (0.749–0.844)	<0.001	>11	73.8 (65.7–80.8)	73.1 (69.7–76.3)	0.797 (0.768–0.823)	<0.001	ns

AUC: area under the curve; CAD: coronary artery disease; MPI: myocardial perfusion imaging; ROC: receiver operating characteristic; SEN: sensitivity %; SPE: specificity %; SSS: summed stress score.
* Comparison with diagonal.
^ Pairwise comparison between the AUCs obtained from ROC analysis in women and men.

we reported such a mismatch only in 73 patients (6% of the overall population); after having excluded image quality issues, it can be reasonably assumed the coexistence of some functional alteration of microcirculation, due to the presence of older age and high prevalence of dyslipidaemia (in women) and arterial hypertension (in men). Therefore, the introduction of cardiac cameras equipped with CZT detectors may help physicians in clinical arena thanks to higher sensitivity and energy resolution compared to conventional SPECT [8]. Interestingly, this study showed a high level of accuracy in detecting one-, two- and three-vessel CAD also in female population, without a significant difference with men. These results are of utmost importance, if we consider many reports stated women consistently receive less intensive medical care and are under-referred to cardiovascular imaging procedures [2,23]. This is partially because women commonly present with more atypical, less exertional symptoms, which confound candidate selection and accurate assessment of pre-test risk [22]. At the same time, there are also technical reasons for this gender-related gap, notably safety issues and poorer diagnostic accuracy, above all with standard SPECT scans [21,22]. Reducing radiation exposure represents one of the main features of CZT-based cardiac imaging, without limiting diagnostic accuracy [16]. Other technical limitations of standard myocardial SPECT were related to soft-tissue attenuation (e.g. breast tissue) and inaccurate left ventricle reconstructions, above all in smaller hearts [24]. These gaps were more typical of ^{201}Tl and have been partially overcome with higher energy ^{99m}Tc radioisotopes and gated SPECT [23]. CZT cameras come as a further breakthrough in terms of spatial resolution and consequent identification of stress defects, thanks to its original design of the detector [25]. All these reasons may explain the high MPI accuracy demonstrated in our study, irrespective also of the stress protocol: exercise stress test or dipyridamole stress (supplemental material). Noteworthy, in female and male population submaximal exercise was associated with a non-significant lower accuracy in detecting CAD, in comparison both to maximal exercise and dipyridamole stress. The underperformance of a submaximal exercise was significant in men with multi-vessel CAD when compared with maximal exercise, but not in comparison with dipyridamole stress. This disappointing result can be at least in part reduced if we consider only one patient out of four was unable to perform a maximal exercise. On the contrary, more than one third of women did not achieve maximal heart rate (above all due to a higher prevalence of overweight and/or orthopedic limitations), but nevertheless CZT-based MPI proved to be reliable for the diagnosis of single-vessel and multi-vessel CAD.

Finally, the multipinhole technique provided by CZT cameras improves accuracy in LV volume and mass reconstruction, together with volume curve analysis during the cardiac cycle. In fact, LV morpho-functional evaluation significantly distinguished women from men, as previously described [2,13,26]. A coherent and significant patient stratification was demonstrated also after the division into subgroups, according to the number of vessels with CAD. Particularly in comparison with single-vessel CAD, patients with multi-vessel CAD had a significant higher impairment of systolic and diastolic function, along with a more advanced LV remodeling. Then, these parameters can be described as additional tricks up the physician's sleeve when requesting a CZT-SPECT scan.

5. Study limitations

The consecutive nature of the enrolment prevented the selection of a homogeneous population; indeed, female subjects were about a third of male patients. Fractional flow reserve measurement during coronary catheterization was not available in all the patients, therefore we used quantitative coronary angiography.

While the present population may partially overlap with the population of patients of previous reports (371/1161, 31%) [4,6], the larger number of patients as well as study variables and end-points between the present and previous reports ensure the originality of the data. The lack of CT attenuation correction may represent a limit of the protocol, affecting diagnostic accuracy of the study. Nevertheless, our protocol included a thorough morpho-functional evaluation (e.g. LV mass, diastolic function, LV remodeling) in addition to conventional MPI to limit any potential gap in diagnostic accuracy and it allowed us to minimize radiation dose. Larger and multi-center studies are needed to validate the incremental value of CT attenuation correction, as well as PFR and LV EI. Patients analysed in this study showed a low occurrence of ventricular dysfunction, and thus our findings may be not representative of dilated hearts.

6. Conclusion

Evaluation of multivessel disease can be obtained by CZT camera in men as well as in women with high accuracy. The CZT low-dose protocol is of utmost importance especially for women, because a lower radiation exposure of the patients is associated with a better safety, but it does not come at the expense of a lower accuracy, even in the presence of multi-vessel CAD and submaximal exercise stress. As a bonus, CZT-based MPI provides a morpho-functional analysis to further discriminate patients with different degrees of CAD.

Funding

This research received no specific grant.

Conflict of interest

All the authors declare no conflict of interests.

Ethical approval

The study was conducted in accordance with the ethical standards of the institutional research committee and with the 1964 Helsinki declaration.

Informed consent

Informed consent was obtained from all individual participants included in the study.

References

[1] E.J. Benjamin, S.S. Virani, C.W. Callaway, A.R. Chang, S. Cheng, S.E. Chiuve, M. Cushman, F.N. Delling, R. Deo, S.D. de Ferranti, J.F. Ferguson, M. Fornage, C. Gillespie, C.R. Isasi, M.C. Jiménez, L.C. Jordan, S.E. Judd, D. Lackland, J.H. Lichtman, L. Lisabeth, S. Liu, C.T. Longenecker, P.L. Lutsey, D.B. Matchar, K. Matsushita, M.E. Mussolino, K. Nasir, M. O'Flaherty, L.P. Palaniappan, D.K. Pandey, M.J. Reeves, M.D. Ritchey, C.J. Rodriguez, G.A. Roth, W.D. Rosamond, U.K.A. Sampson, G.M. Satou, S.H. Shah, N.L. Spartano, D.L. Tirschwell, C.W. Tsao, J.H. Voeks, J.Z. Willey, J.T. Wilkins, J.H. Wu, H.M. Alger, S.S. Wong, P. Muntner, Heart Disease and Stroke Statistics—2018 Update: A Report From the American Heart Association, 2018, https://doi.org/10.1161/CIR.0000000000000558.

[2] R. Hachamovitch, D.S. Berman, H. Kiat, C.N. Bairey Merz, I. Cohen, J.A. Cabico, J. Friedman, G. Germano, K.F. Van Train, G.A. Diamond, Effective risk stratification using exercise myocardial perfusion SPECT in women: gender-related differences in prognostic nuclear testing, J. Am. Coll. Cardiol. 28 (1996) 34–44.

[3] C. Santana-Boado, J. Candell-Riera, J. Castell-Conesa, S. Aguadé-Bruix, A. García-Burillo, T. Canela, J.M. González, J. Cortadellas, D. Ortega, J. Soler-Soler, Diagnostic accuracy of technetium-99m-MIBI myocardial SPECT in women and men, J. Nucl. Med. 39 (1998) 751–755.

[4] A. Gimelli, M. Bottai, A. Quaranta, A. Giorgetti, D. Genovesi, P. Marzullo, Gender differences in the evaluation of coronary artery disease with a cadmium-zinc telluride camera, Eur. J. Nucl. Med. Mol. Imaging 40 (2013) 1542–1548.

[5] R.T. George, V.C. Mehra, M.Y. Chen, K. Kitagawa, A. Arbab-Zadeh, J.M. Miller, M.B. Matheson, A.L. Vavere, K.F. Kofoed, C.E. Rochitte, M. Dewey, T.S. Yaw, H. Niinuma, W. Brenner, C. Cox, M.E. Clouse, J.A.C. Lima, M. Di Carli, Myocardial CT perfusion imaging and SPEC T for the diagnosis of coronary artery disease: a head-to-head comparison from the CORE320 multicenter diagnostic performance study, Radiology 272 (2014) 407–416.

[6] A. Gimelli, R. Liga, V. Duce, A. Kusch, A. Clemente, P. Marzullo, Accuracy of myocardial perfusion imaging in detecting multivessel coronary artery disease: a cardiac CZT study, J. Nucl. Cardiol. 24 (2017) 687–695.

[7] M. Kaminek, I. Metelkova, M. Budikova, P. Koranda, L. Henzlova, M. Havel, E. Sovova, V. Kincl, Diagnosis of high-risk patients with multivessel coronary artery disease by combined cardiac gated SPET imaging and coronary calcium score, Hell. J. Nucl. Med. 18 (2015) 31–34.

[8] S. Yokota, M. Mouden, J.P. Ottervanger, High-risk coronary artery disease, but normal myocardial perfusion: a matter of concern? J. Nucl. Cardiol. 23 (2016) 542–545.

[9] B.A. Herzog, R.R. Buechel, R. Katz, M. Brueckner, L. Husmann, I.A. Burger, A.P. Pazhenkottil, I. Valenta, O. Gaemperli, V. Treyer, P.A. Kaufmann, Nuclear myocardial perfusion imaging with a cadmium-zinc-telluride detector technique: optimized protocol for scan time reduction, J. Nucl. Med. 51 (2010) 46–51.

[10] A. Gimelli, R. Liga, M. Bottai, E.M. aria Pasanisi, A. Giorgetti, S. Fucci, P. Marzullo, Diastolic dysfunction assessed by ultra-fast cadmium-zinc-telluride cardiac imaging: impact on the evaluation of ischaemia, Eur. Heart J. Cardiovasc. Imaging 16 (2015) 68–73.

[11] N. Mahajan, L. Polavaram, H. Vankayala, B. Ference, Y. Wang, J. Ager, J. Kovach, L. Afonso, Diagnostic accuracy of myocardial perfusion imaging and stress echocardiography for the diagnosis of left main and triple vessel coronary artery disease: a comparative meta-analysis, Heart 96 (2010) 956–966.

[12] D.S. Berman, X. Kang, P.J. Slomka, J. Gerlach, L. de Yang, S.W. Hayes, J.D. Friedman, L.E.J. Thomson, G. Germano, Underestimation of extent of ischemia by gated SPECT myocardial perfusion imaging in patients with left main coronary artery disease, J. Nucl. Cardiol. 14 (2007) 521–528.

[13] R.S.L. Lima, D.D. Watson, A.R. Goode, M.S. Siadaty, M. Ragosta, G.A. Beller, H. Samady, Incremental value of combined perfusion and function over perfusion alone by gated SPECT myocardial perfusion imaging for detection of severe three-vessel coronary artery disease, J. Am. Coll. Cardiol. 42 (2003) 64–70.

[14] N.H. Lopes, F. da S. Paulitsch, A.F. Gois, A.C. Pereira, N.A. Stolf, L.O. Dallan, J.A.F. Ramires, W.A. Hueb, Impact of number of vessels disease on outcome of patients with stable coronary artery disease: 5-year follow-up of the medical, angioplasty, and bypass surgery study (MASS), Eur. J. Cardio-Thoracic Surg. 33 (2008) 349–354.

[15] R.J. Gibbons, G.J. Balady, J.T. Bricker, B.R. Chaitman, G.F. Fletcher, V.F. Froelicher, D.B. Mark, B.D. McCallister, A.N. Mooss, M.G. O'Reilly, W.L. Winters, R.J. Gibbons, E.M. Antman, J.S. Alpert, D.P. Faxon, V. Fuster, G. Gregoratos, L.F. Hiratzka, A.K. Jacobs, R.O. Russell, S.C. Smith, American College of Cardiology/American Heart Association Task Force on Practice Guidelines, Committee to update the 1997 exercise testing guidelines, ACC/AHA 2002 guideline update for exercise testing: summary article. A report of the American College of Cardiology/American Heart Association Task Force on Practice Guidelines (Committee to Update the 1997 Exercise Testing Guidelines), J. Am. Coll. Cardiol. 40 (2002) 1531–1540.

[16] A. Gimelli, M. Bottai, D. Genovesi, A. Giorgetti, F. Di Martino, P. Marzullo, High diagnostic accuracy of low-dose gated-SPECT with solid-state ultrafast detectors: preliminary clinical results, Eur. J. Nucl. Med. Mol. Imaging 39 (2012) 83–90.

[17] M.D. Cerqueira, N.J. Weissman, V. Dilsizian, A.K. Jacobs, S. Kaul, W.K. Laskey, D.J. Pennell, J.A. Rumberger, T. Ryan, M.S. Verani, American Heart Association Writing Group on Myocardial Segmentation and Registration for Cardiac Imaging, Standardized myocardial segmentation and nomenclature for tomographic imaging of the heart. A statement for healthcare professionals from the Cardiac Imaging Committee of the Council on Clinical Cardiology of the American Heart Association, Circulation 105 (2002) 539–542.

[18] T. Sharir, D.S. Berman, P.B. Waechter, J. Areeda, P.B. Kavanagh, J. Gerlach, X. Kang, G. Germano, Quantitative analysis of regional motion and thickening by gated myocardial perfusion SPECT: normal heterogeneity and criteria for abnormality, J. Nucl. Med. 42 (2001) 1630–1638.

[19] S. Kurisu, Y. Sumimoto, H. Ikenaga, N. Watanabe, K. Ishibashi, Y. Dohi, T. Hidaka, Y. Fukuda, Y. Kihara, Effects of left ventricular size on the accuracy of diastolic parameters derived from myocardial perfusion SPECT: comparison with tissue Doppler echocardiography, Ann. Nucl. Med. 30 (2016) 645–651.

[20] A. Gimelli, R. Liga, A. Clemente, G. Marras, A. Kusch, P. Marzullo, Left ventricular eccentricity index measured with SPECT myocardial perfusion imaging: an additional parameter of adverse cardiac remodeling, J. Nucl. Cardiol. (2017), https://doi.org/10.1007/s12350-017-0777-3.

[21] H.J. Verberne, W. Acampa, C. Anagnostopoulos, J. Ballinger, F. Bengel, P. De Bondt, R.R. Buechel, A. Cuocolo, B.L.F. van Eck-Smit, A. Flotats, M. Hacker, C. Hindorf, P.A. Kaufmann, O. Lindner, M. Ljungberg, M. Lonsdale, A. Manrique, D. Minarik, A.J.H.A. Scholte, R.H.J.A. Slart, E. Trägårdh, T.C. de Wit, B. Hesse, European Association of Nuclear Medicine (EANM), EANM procedural guidelines for radionuclide myocardial perfusion imaging with SPECT and SPECT/CT: 2015 revision, Eur. J. Nucl. Med. Mol. Imaging 42 (2015) 1929–1940.

[22] G. Montalescot, U. Sechtem, S. Achenbach, F. Andreotti, C. Arden, A. Budaj, R. Bugiardini, F. Crea, T. Cuisset, C. Di Mario, J.R. Ferreira, B.J. Gersh, A.K. Gitt, J.-S. Hulot, N. Marx, L.H. Opie, M. Pfisterer, E. Prescott, F. Ruschitzka, M. Sabaté, R. Senior, D.P. Taggart, E.E. van der Wall, C.J.M. Vrints, J.L. Zamorano, H. Baumgartner, J.J. Bax, H. Bueno, V. Dean, C. Deaton, C. Erol, R. Fagard, R. Ferrari, D. Hasdai, A.W. Hoes, P. Kirchhof, J. Knuuti, P. Kolh, P. Lancellotti, A. Linhart, P. Nihoyannopoulos, M.F. Piepoli, P. Ponikowski, P.A. Sirnes, J.L. Tamargo, M. Tendera, A. Torbicki, W. Wijns, S. Windecker, M. Valgimigli, M.J. Claeys, N. Donner-Banzhoff, H. Frank, C. Funck-Brentano, O. Gaemperli, J.R. Gonzalez-Juanatey, M. Hamilos, S. Husted, S.K. James, K. Kervinen, S.D. Kristensen, A. Pietro Maggioni, A.R. Pries, F. Romeo, L. Rydén, M.L. Simoons, P.G. Steg, A. Timmis, A. Yildirir, 2013 ESC guidelines on the management of stable coronary artery disease: the task force on the management of stable coronary artery disease of the European Society of Cardiology, Eur. Heart J. 34 (2013) 2949–3003.

[23] R. Taillefer, E.G. Depuey, J.E. Udelson, G.A. Beller, Y. Latour, F. Reeves, Comparative diagnostic accuracy of Tl-201 and Tc-99m sestamibi SPECT imaging (perfusion and ECG-gated SPECT) in detecting coronary artery disease in women, J. Am. Coll. Cardiol. 29 (1997) 69–77.

[24] G.C. Kane, B.L. Karon, D.W. Mahoney, M.M. Redfield, V.L. Roger, J.C. Burnett, S.J. Jacobsen, R.J. Rodeheffer, Progression of left ventricular diastolic dysfunction and risk of heart failure, JAMA 306 (2011) 856–863.

[25] A. Gimelli, M. Bottai, A. Giorgetti, D. Genovesi, A. Kusch, A. Ripoli, P. Marzullo, Comparison between ultrafast and standard single-photon emission CT in patients with coronary artery disease a pilot study, Circ. Cardiovasc. Imaging 4 (2011) 51–58.

[26] A. Gimelli, R. Liga, A. Giorgetti, A. Kusch, E.M. Pasanisi, P. Marzullo, Relationships between myocardial perfusion abnormalities and poststress left ventricular functional impairment on cadmium-zinc-telluride imaging, Eur. J. Nucl. Med. Mol. Imaging 42 (2015) 994–1003.